Diffusion influence on Michaelis–Menten kinetics: II. The low substrate concentration limit

2007 J. Phys.: Condens. Matter 19 065137

(http://iopscience.iop.org/0953-8984/19/6/065137)

INSTITUTE OF PHYSICS PUBLISHING JOURNAL OF PHYSICS: CONDENSED MATTER

J. Phys.: Condens. Matter **19** (2007) 065137 (13pp) doi:10.1088/0953-8984/19/6/065137

Diffusion influence on Michaelis–Menten kinetics: II. The low substrate concentration limit

Hyojoon Kim[1] **and Kook Joe Shin**

Department of Chemistry, Seoul National University, Seoul 151-747, Korea

E-mail: shinkj@snu.ac.kr

Received 27 July 2006
Published 22 January 2007
Online at stacks.iop.org/JPhysCM/19/065137

Abstract

The diffusion-influenced Michaelis–Menten kinetics in the low substrate concentration limit is studied in one and three dimensions. For the initial pair distribution of enzyme and substrate, we obtain the exact analytical results. We find that at short times the diffusion effect can make the reaction rate faster. The concentration deviations of the substrate and enzyme show $t^{-1/2}$ and $t^{-3/2}$ power-law behaviours in one and three dimensions, respectively, at long times. On the other hand, the average lifetime of the intermediate is independent of the initial state in one dimension, while it depends on the initial state in three dimensions. The ultimate production yield approaches unity in one dimension but it reaches a different value depending on other parameters in three dimensions. We also obtain the analytical results for the initial random distribution.

1. Introduction

The Michaelis–Menten (MM) kinetics [1, 2] has been employed in a wide variety of research fields in chemistry and biology as one of the prototypical reaction models in the enzyme kinetics [3]. Recently, a single-molecule MM kinetics has drawn much attention to describe single-molecule enzyme dynamics [4–6]. The MM scheme can be expressed as

$$\mathrm{E} + \mathrm{S} \underset{k_{-1}}{\overset{k_1}{\rightleftharpoons}} \mathrm{ES} \xrightarrow{k_2} \mathrm{E} + \mathrm{P}, \tag{1}$$

where E, S, ES and P represent enzyme, substrate, intermediate and product, respectively, and k_i denotes the corresponding reaction rate coefficient. The classical MM kinetics is based on two main approximations: the assumption that the rate coefficients are independent of time and the steady-state approximation. The former approximation becomes invalid when the reaction is strongly influenced by diffusion. Since reactants should be encountered for a reaction to

[1] Present address: Department of Chemistry, University of Toronto, Toronto, ON, M5S 1A1, Canada.

occur, diffusion effects are likely to be more pronounced in *in vivo* than *in vitro* conditions where the system can be easily well mixed. It is well known that the diffusion-influenced reaction strongly depends on the dimensionality of the system and the heterogeneity of the media [7]. Therefore, biological reactions in a low-dimensional medium like membrane [8–11] or in a heterogeneous cellular medium [12] are difficult to elucidate using the classical MM kinetics. Since diffusion is a many-body problem *per se* and the exact analytical solutions are rare, one usually has to rely on numerical methods [13–15] or computer simulations [11, 16, 17] to tackle the diffusion-influenced reaction problems.

Some time ago, Zhou [18] reported that the influence of diffusion on the MM kinetics leads to a nonlinearity in the Lineweaver–Burk (LB) plot [3] for high substrate concentrations based on an empirical formula. Later, Kim *et al* applied the renormalized kinetic theory [19] to the MM kinetics and confirmed the LB nonlinearity systematically [20]. By ordinary perturbation methods in the absence of diffusion, Murugan found the LB nonlinearity, which is ascribed to the effect of transient dynamics [21].

The long time asymptotic behaviour of the MM kinetics in the presence of diffusion shows $t^{-1/2}$ power law behaviour [20], contrary to the well known $t^{-3/2}$ law for the $\mathrm{A}+\mathrm{B}\rightleftarrows\mathrm{C}$ system. By using a fluctuation theory approach, Paul and Gangopadhyay [22] reported that the asymptotic behaviour obeys the $t^{-3/2}$ law if the second step of the MM kinetics is assumed to be reversible.

In the classical MM kinetics neglecting diffusion effects, we can solve the following coupled differential equations:

$$\frac{\mathrm{d}[\mathrm{E}]}{\mathrm{d}t} = -\frac{\mathrm{d}[\mathrm{ES}]}{\mathrm{d}t} = -k_1[\mathrm{E}][\mathrm{S}] + (k_{-1}+k_2)[\mathrm{ES}], \tag{2}$$

$$\frac{\mathrm{d}[\mathrm{S}]}{\mathrm{d}t} = -k_1[\mathrm{E}][\mathrm{S}] + k_{-1}[\mathrm{S}], \tag{3}$$

$$\frac{\mathrm{d}[\mathrm{P}]}{\mathrm{d}t} = k_2[\mathrm{ES}]. \tag{4}$$

Numerous theoretical efforts have been devoted to describing the dynamics more correctly [23–28]. Since these equations are not solvable analytically, the steady-state approximation of $\mathrm{d}[\mathrm{ES}]/\mathrm{d}t \sim 0$ is introduced [2]. The steady-state approximation is valid when one reactant concentration is much higher than the other, such as $[\mathrm{E}]_0 \ll [\mathrm{S}]_0 + K_M$ or $[\mathrm{S}]_0 \ll [\mathrm{E}]_0 + K_M$, where the subscript 0 denotes the initial concentration and $K_M = (k_{-1}+k_2)/k_1$ [28].

In this way, the limitations of the classical MM kinetics can be too significant to ignore when $[\mathrm{E}]_0 \approx [\mathrm{S}]_0$ with the strong diffusion effect [29]. When $[\mathrm{E}]_0 \approx [\mathrm{S}]_0$, it is difficult to obtain rigorous analytical results even with the most advanced theories in the diffusion–reaction fields. However, in the low [S] limit, we can solve the MM kinetics *exactly*, even including the diffusion effect, since the competition among substrates can be neglected in this limit by effectively circumventing the many-body problem.

The purpose of this paper is to provide exact analytical results in the low [S] limit in the cases where the classical MM kinetics fails. Exact analytical results are important not only because they can give a crucial theoretical reference to other problems as a special or limiting case but also because they can be used to devise efficient many-body Brownian dynamics simulation algorithms [16, 30]. These simulation methods have been successful in obtaining the numerically exact data in various reversible diffusion-influenced reactions [31, 32]. In addition to the fact that the present analytical results can be useful to directly explain various interesting biological phenomena observed at low substrate concentrations [33–35], the exact results can be used to open the door to obtain the numerically exact data for a general MM kinetics.

The initial pair distribution of enzyme and substrate is usually not localized but random in the MM kinetics. We also present the analytical results for this random distribution. Since the intra-pair reaction region is well separated from the inter-pair one in the low [S] limit [36], an enzyme molecule can be assumed to react with its nearest neighbour substrate molecule.

By Polya's theorem [37], which states that the random walker always returns to its starting point when the system dimension is less than two, three-dimensional diffusion effects often show qualitative differences from low dimensional effects. For this reason, we present the results in one dimension (1D) as well as those in three dimensions (3D) and also discuss differences between the two of them.

2. Exact results

Consider a diffusing pair of spherical molecules of enzyme (E) and substrate (S) with a relative diffusion constant D ($=D_{\mathrm{E}} + D_{\mathrm{S}}$). The reaction between the pair obeys the mechanism of equation (1). From the normalized mass conservation law, we obtain the following relations:

$$\begin{aligned} &[\mathrm{S}] + [\mathrm{ES}] + [\mathrm{P}] = [\mathrm{S}]_0 + [\mathrm{ES}]_0 \equiv 1, \\ &[\mathrm{E}] + [\mathrm{ES}] = [\mathrm{E}]_0 + [\mathrm{ES}]_0 \equiv 1. \end{aligned} \tag{5}$$

The bimolecular association reaction can occur instantaneously when two molecules approach within a reaction distance σ. Let $p(r, t)$ be the probability that S is separated by a distance r from E at time t. Then the time evolution of $p(r, t)$ can be described by the following field-free diffusion equation in d dimensions:

$$\frac{\partial p(r,t)}{\partial t} = D\left(\frac{\partial^2}{\partial r^2} + \frac{d-1}{r}\frac{\partial}{\partial r}\right) p(r,t). \tag{6}$$

The evolution equation of the intermediate [ES] is given by

$$\frac{\partial [\mathrm{ES}]}{\partial t} = k_1 p(\sigma, t) - (k_{-1} + k_2)\,[\mathrm{ES}]. \tag{7}$$

Moreover, the boundary conditions for equation (6) are given by

$$\begin{aligned} &C_d(\sigma) D \left.\frac{\partial p(r,t)}{\partial r}\right|_{r=\sigma} = k_1 p(\sigma, t) - (k_{-1} + k_2)\,[\mathrm{ES}], \\ &\lim_{r\to\infty} p(r,t) = 0, \end{aligned} \tag{8}$$

where $C_d(r)$ is unity for 1D and $4\pi r^2$ for 3D.

The concentrations of the substrate and the product can be calculated by

$$[\mathrm{S}] = \int_{\sigma}^{\infty} C_d(r)\, p(r,t)\, \mathrm{d}r, \tag{9}$$

$$[\mathrm{P}] = k_2 \int_0^t \mathrm{d}t [\mathrm{ES}], \tag{10}$$

respectively. Note that [P] can be also calculated from equation (5) once we know [S] and [ES]. In this work, we treat only the case of $[\mathrm{S}]_0 = [\mathrm{E}]_0$ since the contribution to the reaction of the excess concentration of S or E is negligible in the low concentration limit.

A pair of enzyme and substrate molecules can be initially in the bound (ES) or unbound (E + S) state. Let $[\alpha]^{r_0}$ denote the concentration of α species at time t for an initial *unbound* state for which E is initially separated from S by a separation r_0 and $[\alpha]^*$ for E and S in an initial *bound* state.

The average lifetimes of ES may be defined as

$$\tau^* \equiv \int_0^\infty \mathrm{d}t[\mathrm{ES}]^*, \tag{11}$$

$$\tau^{r_0} \equiv \int_0^\infty \mathrm{d}t[\mathrm{ES}]^{r_0}, \tag{12}$$

for the initial bound and unbound states, respectively. The concentration of E for an arbitrary initial distribution $p(r_0)$ can be obtained by

$$[\mathrm{E}] = \int_\sigma^\infty [\mathrm{E}]_0 p(r_0)[\mathrm{E}]^{r_0} C_d(r_0)\,\mathrm{d}r_0 + [\mathrm{ES}]_0[\mathrm{E}]^*. \tag{13}$$

The above evolution equations (equations (6)–(8)) can be solved exactly by the methods developed for the following excited-state reversible geminate reaction with two lifetimes:

$$\begin{array}{lll} \mathrm{A}^* + \mathrm{B} \underset{k_d}{\overset{k_a}{\rightleftharpoons}} & \mathrm{C}^* \\ \downarrow k_0' & \downarrow k_0 \\ \mathrm{A} & \mathrm{C} \end{array} \tag{14}$$

in 3D [38, 39] and in 1D [40], respectively. The theoretical predictions were confirmed experimentally [41, 42]. One can see the similarities between equations (1) and (14). In this paper, we present only the results obtained as follows. First, one can obtain the Green function $p(r, t)$ for the initial unbound state by solving the coupled differential equations with the aid of the Laplace transformation technique. Then the integration of $p(r, t)$ using equation (9) gives [S]. [ES] and, therefore, [P] can be calculated from equations (7) and (10), respectively. For the initial bound state, the corresponding concentrations can be obtained by utilizing the detailed balance equation.

2.1. One dimension

The results in 1D can be directly obtained from [40] by making corresponding changes such as $\mathrm{A}^* \to \mathrm{E}$, $\mathrm{B} \to \mathrm{S}$, $\mathrm{C}^* \to \mathrm{ES}$, $\mathrm{C} \to \mathrm{P}$, $k_a \to k_1$, $k_d \to k_{-1}$, $k_0' \to 0$, and $k_0 \to k_2$ to give

$$[\mathrm{ES}]^{r_0} = \frac{k_1}{D}\sum_{i=1}^{3} \alpha_i \Phi_{ijk}\,(r_0 - \sigma), \tag{15}$$

$$[\mathrm{ES}]^* = \sum_{i=1}^{3} \alpha_i(\alpha_j + \alpha_k)\Phi_{ijk}\,(0), \tag{16}$$

$$[\mathrm{S}]^{r_0} = \mathrm{erf}\left(\frac{r_0 - \sigma}{2\sqrt{Dt}}\right) - \sum_{i=1}^{3} (\alpha_k + \alpha_i)(\alpha_i + \alpha_j)\Phi_{ijk}\,(r_0 - \sigma), \tag{17}$$

$$[\mathrm{S}]^* = -\frac{k_{-1}}{D}\sum_{i=1}^{3} \Phi_{ijk}(0), \tag{18}$$

$$[\mathrm{P}]^{r_0} = \mathrm{erfc}\left(\frac{r_0 - \sigma}{2\sqrt{Dt}}\right) + \frac{k_1 k_2}{D^2}\sum_{i=1}^{3} \frac{1}{\alpha_i}\Phi_{ijk}\,(r_0 - \sigma), \tag{19}$$

$$[\mathrm{P}]^* = 1 + \frac{k_2}{D}\sum_{i=1}^{3} \frac{(\alpha_j + \alpha_k)}{\alpha_i}\Phi_{ijk}\,(0), \tag{20}$$

where $i \neq j \neq k = 1, 2, 3$. The error function and its complementary are denoted as $\mathrm{erf}(x)$ and $\mathrm{erfc}(x)$, respectively. α_i is one of the roots of the following set of coupled equations:

$$\begin{aligned} &\alpha_1 + \alpha_2 + \alpha_3 = k_1/D, \\ &\alpha_1\alpha_2 + \alpha_2\alpha_3 + \alpha_3\alpha_1 = (k_2 + k_{-1})/D, \\ &\alpha_1\alpha_2\alpha_3 = k_1k_2/D^2. \end{aligned} \tag{21}$$

$\Phi_{ijk}(r)$ is defined as

$$\begin{aligned} &\Phi_{ijk}(r) = \frac{1}{(\alpha_k - \alpha_i)(\alpha_i - \alpha_j)} W\left(\frac{r}{2\sqrt{Dt}}, \alpha_i\sqrt{Dt}\right), \\ &W(a, b) = \exp\left(2ab + b^2\right)\mathrm{erfc}(a + b). \end{aligned} \tag{22}$$

Note that $W(0, \alpha_i\sqrt{Dt}) = \exp(\alpha_i^2 Dt)\mathrm{erfc}(\alpha_i\sqrt{Dt})$. We omit the expressions for [E] because they can be easily obtained from those for [ES] using equation (5). One can check that the steady-state approximation does not hold because [ES] does not become constant.

Using the integral formulae

$$\int_0^\infty \mathrm{d}t \sum_{i=1}^{3} \alpha_i(\alpha_j + \alpha_k)\Phi_{ijk}(0) = \frac{1}{D}\frac{\alpha_1 + \alpha_2 + \alpha_3}{\alpha_1\alpha_2\alpha_3}, \tag{23}$$

$$\int_0^\infty \mathrm{d}t \sum_{i=1}^{3} \alpha_i\Phi_{ijk}(r) = \frac{1}{D}\frac{1}{\alpha_1\alpha_2\alpha_3}, \tag{24}$$

the average lifetimes of ES can be obtained from equations (11) and (12) to give

$$\tau^* = \tau^{r_0} = \tau = 1/k_2. \tag{25}$$

Interestingly, the lifetime τ is independent of the initial state and is dependent only on k_2 in 1D.

2.2. Three dimensions

As in 1D, the results in 3D can be directly obtained from [39] to give

$$[\mathrm{ES}]^{r_0} = \frac{k_1}{r_0 k_D}\sum_{i=1}^{3}\alpha_i\Phi_{ijk}(r_0 - \sigma), \tag{26}$$

$$[\mathrm{ES}]^{*} = \sum_{i=1}^{3}\alpha_i(\alpha_j + \alpha_k)\Phi_{ijk}(0), \tag{27}$$

$$\begin{aligned} [\mathrm{S}]^{r_0} = 1 - \frac{\sigma}{r_0}\left(1 - [\mathrm{S}]_\infty^\sigma\right)\mathrm{erfc}\left(\frac{r_0 - \sigma}{2\sqrt{Dt}}\right) \\ + \frac{\sigma}{r_0}\sum_{i=1}^{3}\left(\frac{1}{\sigma\alpha_i} - 1\right)(\alpha_k + \alpha_i)(\alpha_i + \alpha_j)\Phi_{ijk}(r_0 - \sigma), \end{aligned} \tag{28}$$

$$[\mathrm{S}]^{*} = [\mathrm{S}]_\infty^{*} + \frac{k_{-1}}{D}\sum_{i=1}^{3}\left(\frac{1}{\sigma\alpha_i} - 1\right)\Phi_{ijk}(0), \tag{29}$$

$$[\mathrm{P}]^{r_0} = \frac{\sigma}{r_0}\left(1 - [\mathrm{S}]_\infty^\sigma\right)\mathrm{erfc}\left(\frac{r_0 - \sigma}{2\sqrt{Dt}}\right) + \frac{k_1k_2}{r_0k_DD}\sum_{i=1}^{3}\frac{1}{\alpha_i}\Phi_{ijk}(r_0 - \sigma), \tag{30}$$

$$[\mathrm{P}]^{*} = 1 - [\mathrm{S}]_\infty^{*} + \frac{k_2}{D}\sum_{i=1}^{3}\frac{(\alpha_j + \alpha_k)}{\alpha_i}\Phi_{ijk}(0), \tag{31}$$

where α_i is one of the roots of the following set of coupled equations different from those in 1D:

$$\begin{aligned}
&\alpha_1+\alpha_2+\alpha_3=(1+k_1/k_D)/\sigma,\\
&\alpha_1\alpha_2+\alpha_2\alpha_3+\alpha_3\alpha_1=(k_2+k_{-1})/D,\\
&\alpha_1\alpha_2\alpha_3=\left[k_2(1+k_1/k_D)+k_{-1}\right]/(D\sigma),
\end{aligned} \tag{32}$$

where $k_D \equiv 4\pi\sigma D$. The definitions of $[\mathrm{S}]^*_\infty$ and $[\mathrm{S}]^\sigma_\infty$ are given by

$$[S]^*_\infty = \frac{k_{-1}}{k_{-1}+k_2(1+k_1/k_D)}, \tag{33}$$

$$[S]^\sigma_\infty = \frac{k_2+k_{-1}}{k_{-1}+k_2(1+k_1/k_D)}, \tag{34}$$

where the subscript ∞ denotes the long time value.

The expressions for various concentrations in 3D are very similar to those in 1D. The expressions for [ES] are the same as those in 1D and those for [P] show the same expressions except the $[\mathrm{S}]_\infty$ term and the factor of σ/r_0. On the other hand, the expressions for [S] are somewhat different because they are obtained by the integration with respect to different volume elements (equation (9)).

Using equations (23) and (24), the average lifetimes of ES in 3D for the initial bound and unbound states can be obtained, respectively, as

$$\tau^* = \frac{1+k_1/k_D}{k_2(1+k_1/k_D)+k_{-1}}, \tag{35}$$

$$\tau^{r_0} = \frac{\sigma}{r_0}\frac{k_1/k_D}{k_2(1+k_1/k_D)+k_{-1}}. \tag{36}$$

By comparing these results with equation (25), we can observe two distinctive features in the lifetimes of ES in 3D: One is $\tau^* \neq \tau^{r_0}$, which comes from the fact that the escape probability is not zero in 3D. The other is that τ depends not only on k_2 but also on k_1, k_{-1}, and k_D.

3. Solutions for random initial distribution

The initial distribution of enzyme and substrate molecules is usually the Poisson distribution rather than the localized one. Utilizing equation (13), we can obtain the probability functions for the random initial distribution, $p(r_0) = \exp\{-V_d(r_0)[\mathrm{E}]_0\}$, where $V_d(r)$ is r for 1D and $(4/3)\pi r^3$ for 3D. Unlike the localized distribution, the random one depends on the initial concentration $[\mathrm{E}]_0$ or $[\mathrm{S}]_0$ since the separated distance is larger at lower concentration. For instance, [E] for the random initial distribution can be calculated by

$$[\mathrm{E}]^{\mathrm{ran}} = \int_0^\infty \mathrm{d}r_0[\mathrm{E}]_0 C_d(r_0)\exp\{-V_d(r_0)[\mathrm{E}]_0\}[\mathrm{E}]^{r_0}. \tag{37}$$

We can obtain the exact closed-form solutions for the random initial distribution in 1D. However, the analytic integrations are not possible in 3D, and we will show the results in 3D only in the low [S] limit.

3.1. Exact results in 1D

In 1D, the results are given by

$$[\mathrm{ES}]^{\mathrm{ran}} = -\frac{k_1}{D}\left(\frac{[\mathrm{S}]_0^2 W\left(0,[\mathrm{S}]_0\sqrt{Dt}\right)}{(\alpha_1-[\mathrm{S}]_0)(\alpha_2-[\mathrm{S}]_0)(\alpha_3-[\mathrm{S}]_0)}+\sum_{i=1}^{3}\frac{\alpha_i[\mathrm{S}]_0\Phi_{ijk}(0)}{\alpha_i-[\mathrm{S}]_0}\right), \tag{38}$$

$$[\mathrm{S}]^{\mathrm{ran}} = \frac{(\alpha_1+\alpha_2+\alpha_3)\,[\mathrm{S}]_0^2+\alpha_1\alpha_2\alpha_3}{(\alpha_1-[\mathrm{S}]_0)\,(\alpha_2-[\mathrm{S}]_0)\,(\alpha_3-[\mathrm{S}]_0)} W\left(0,[\mathrm{S}]_0\sqrt{Dt}\right) + \sum_{i=1}^{3}\frac{(\alpha_k+\alpha_i)(\alpha_i+\alpha_j)[\mathrm{S}]_0}{(\alpha_i-[\mathrm{S}]_0)}\Phi_{ijk}(0), \tag{39}$$

$$[\mathrm{P}]^{\mathrm{ran}} = 1-\frac{\alpha_1\alpha_2\alpha_3 W\left(0,[\mathrm{S}]_0\sqrt{Dt}\right)}{(\alpha_1-[\mathrm{S}]_0)\,(\alpha_2-[\mathrm{S}]_0)\,(\alpha_3-[\mathrm{S}]_0)} - \sum_{i=1}^{3}\frac{\alpha_1\alpha_2\alpha_3[\mathrm{S}]_0}{\alpha_i\,(\alpha_i-[\mathrm{S}]_0)}\Phi_{ijk}(0). \tag{40}$$

3.2. The low [S] *limit*

When there are many pairs in the system, the inter-pair reactions as well as the intra-pair reactions can occur. This competition effect cannot be solved without tackling a many body problem. In the low [S] limit, the competition effect can be neglected and we can obtain the following analytical solutions.

3.2.1. One dimension

$$\lim_{[\mathrm{S}]_0\to 0}[\mathrm{ES}]^{\mathrm{ran}} = -\frac{k_1}{D}[\mathrm{S}]_0\sum_{i=1}^{3}\Phi_{ijk}(0), \tag{41}$$

$$\lim_{[\mathrm{S}]_0\to 0}[\mathrm{S}]^{\mathrm{ran}} = 1-[\mathrm{S}]_0\left[\frac{2\sqrt{Dt}}{\sqrt{\pi}}-\frac{(k_{-1}+k_2)\,D}{k_1k_2}\right]+[\mathrm{S}]_0\sum_{i=1}^{3}\frac{(\alpha_k+\alpha_i)\left(\alpha_i+\alpha_j\right)}{\alpha_i}\Phi_{ijk}(0), \tag{42}$$

$$\lim_{[\mathrm{S}]_0\to 0}[\mathrm{P}]^{\mathrm{ran}} = [\mathrm{S}]_0\left[\frac{2\sqrt{Dt}}{\sqrt{\pi}}-\frac{(k_{-1}+k_2)\,D}{k_1k_2}\right]-[\mathrm{S}]_0\frac{k_1k_2}{D^2}\sum_{i=1}^{3}\frac{\Phi_{ijk}\,(0)}{\alpha_i^2}. \tag{43}$$

3.2.2. Three dimensions

$$\lim_{[\mathrm{S}]_0\to 0}[\mathrm{ES}]^{\mathrm{ran}} = \frac{k_1}{k_{-1}}[\mathrm{S}]_\infty^*[\mathrm{S}]_0+\frac{k_1}{D}[\mathrm{S}]_0\sum_{i=1}^{3}\left(\frac{1}{\sigma\alpha_i}-1\right)\Phi_{ijk}(0), \tag{44}$$

$$\begin{aligned}\lim_{[\mathrm{S}]_0\to 0}[\mathrm{S}]^{\mathrm{ran}} = {} & 1+4\pi\sigma^2[\mathrm{S}]_0\sum_{i=1}^{3}\left(\frac{1}{\sigma\alpha_i}-1\right)^2\frac{(\alpha_k+\alpha_i)\left(\alpha_i+\alpha_j\right)}{\alpha_i}\Phi_{ijk}(0)\\ & -[\mathrm{S}]_0\left(1-[\mathrm{S}]_\infty^\sigma\right)\left[k_Dt+4\pi\sigma^2\left(1-[\mathrm{S}]_\infty^\sigma\right)\left(\frac{2\sqrt{Dt}}{\sqrt{\pi}}-\sigma[\mathrm{S}]_\infty^\sigma\right)\right.\\ & \left.-\frac{k_D}{k_{-1}}[\mathrm{S}]_\infty^*+\frac{k_D}{k_2}[\mathrm{S}]_\infty^\sigma\right],\end{aligned} \tag{45}$$

$$\begin{aligned}\lim_{[\mathrm{S}]_0\to 0}[\mathrm{P}]^{\mathrm{ran}} = {} & [\mathrm{S}]_0\left(1-[\mathrm{S}]_\infty^\sigma\right)\left[k_Dt+4\pi\sigma^2\left(1-[\mathrm{S}]_\infty^\sigma\right)\left(\frac{2\sqrt{Dt}}{\sqrt{\pi}}-\sigma[\mathrm{S}]_\infty^\sigma\right)\right.\\ & \left.-\frac{[\mathrm{S}]_\infty^*}{k_{-1}}(k_D+k_1)\right]+\frac{k_1k_2}{D^2}[\mathrm{S}]_0\sum_{i=1}^{3}\left(\frac{1}{\sigma\alpha_i}-1\right)\frac{\Phi_{ijk}(0)}{\alpha_i^2}.\end{aligned} \tag{46}$$

It should be noted that the results in this subsection can be obtained by taking the low [S] limit of the pseudo-first-order MM kinetics ($[\mathrm{E}]_0 \ll [\mathrm{S}]_0$) described by the renormalized kinetic theory reported earlier [20].

4. Asymptotic results

In the excited-state geminate reaction with two lifetimes, we can observe a kinetic transition behaviour in the long time asymptotic result: the A regime with the power-law relaxation and the AB regime with the exponential behaviour separated by the transition region [39]. For the MM reaction, however, it always obeys the power-law behaviour at long times and no kinetic transition appears. At short and long times, the asymptotic expressions of $\Phi_{ijk}(r)$ can be obtained by using the following asymptotic expressions:

$$\lim_{t\to 0} W\left(\frac{a}{\sqrt{t}}, b\sqrt{t}\right) \sim \operatorname{erfc}\left(\frac{a}{\sqrt{t}}\right), \tag{47}$$

$$\lim_{t\to \infty} W\left(\frac{a}{\sqrt{t}}, b\sqrt{t}\right) \sim \frac{1}{b\sqrt{\pi t}} - \frac{2a^2b^2+1+2ab}{2b^3 t\sqrt{\pi t}}. \tag{48}$$

4.1. Short-time behaviours

At short times, the concentrations for the initial unbound state are zero ($\sim t^{1/2}\exp(-1/t)$) except when $r_0 = \sigma$. We find that the concentrations for the initial bound state in the short time limit show the same expressions for both 1D and 3D as follows:

$$\lim_{t\to 0} [\mathrm{ES}]^* \sim 1 - (k_2 + k_{-1})\, t, \tag{49}$$

$$\lim_{t\to 0} [\mathrm{S}]^* \sim k_{-1} t, \tag{50}$$

$$\lim_{t\to 0} [\mathrm{P}]^* \sim k_2 t. \tag{51}$$

For the initial bound state, the concentrations become the same as those in the classical kinetics without diffusion. This can be explained by the fact that the diffusion effect is not fully developed yet at short times. Therefore, they do not depend on the dimensionality of the system.

For the initial random distribution, the results are

$$\lim_{\substack{[\mathrm{S}]_0\to 0 \\ t\to 0}} [\mathrm{ES}]^{\mathrm{ran}} \sim k_1 [\mathrm{S}]_0 t, \tag{52}$$

$$\lim_{\substack{[\mathrm{S}]_0\to 0 \\ t\to 0}} [\mathrm{S}]^{\mathrm{ran}} \sim 1 - k_1 [\mathrm{S}]_0 t. \tag{53}$$

Again they are the same as in the classical kinetics and independent of the dimensionality.

When $r_0 = \sigma$, the short time asymptotic concentrations for the initial unbound state show different behaviours both in 1D and 3D:

$$\lim_{t\to 0} [\mathrm{ES}]^{\sigma} \sim \frac{2k'_d}{\sqrt{\pi D}} t^{1/2}, \tag{54}$$

$$\lim_{t\to 0} [\mathrm{S}]^{\sigma} \sim 1 - \frac{2k'_d}{\sqrt{\pi D}} t^{1/2}, \tag{55}$$

$$\lim_{t\to 0} [\mathrm{P}]^{\sigma} \sim \frac{4k'_d k_2}{3\sqrt{\pi D}} t^{3/2}, \tag{56}$$

with $k'_d = k_1$ in 1D and $k'_d = k_1/4\pi\sigma^2$ in 3D.

4.2. Long-time behaviours

Although the inter-pair reaction is dominant at very long times, there is a large timescale separation between intra-pair and inter-pair reaction regions at low concentration [36]. Given this timescale separation, we find the long time asymptotic concentrations in 1D and 3D, respectively, as follows:

4.2.1. One dimension

$$\lim_{t\to\infty}[\mathrm{ES}]^{r_0} \sim \left(r_0 - \sigma + \frac{(k_2 + k_{-1})\,D}{k_1 k_2}\right)\frac{1}{2k_2}\frac{1}{\sqrt{D\pi}}t^{-3/2}, \tag{57}$$

$$\lim_{t\to\infty}[\mathrm{ES}]^{*} \sim \frac{k_{-1}}{2k_1k_2^2}\sqrt{\frac{D}{\pi}}t^{-3/2}, \tag{58}$$

$$\lim_{\substack{[\mathrm{S}]_0\to 0\\ t\to\infty}}[\mathrm{ES}]^{\mathrm{ran}} \sim \frac{[\mathrm{S}]_0}{k_2}\frac{\sqrt{D}}{\sqrt{\pi t}}, \tag{59}$$

$$\lim_{t\to\infty}[\mathrm{S}]^{r_0} \sim \left[r_0 - \sigma + \frac{(k_2 + k_{-1})\,D}{k_1 k_2}\right]\frac{1}{\sqrt{D\pi}}t^{-1/2}, \tag{60}$$

$$\lim_{t\to\infty}[\mathrm{S}]^{*} \sim \frac{k_{-1}}{k_1k_2}\sqrt{\frac{D}{\pi}}t^{-1/2}. \tag{61}$$

$$\lim_{\substack{[\mathrm{S}]_0\to 0\\ t\to\infty}}[\mathrm{S}]^{\mathrm{ran}} \sim 1 - \frac{[\mathrm{S}]_0 2\sqrt{Dt}}{\sqrt{\pi}}. \tag{62}$$

4.2.2. Three dimensions

$$\lim_{t\to\infty}[\mathrm{ES}]^{r_0} \sim [\mathrm{S}]_\infty^{r_0}[\mathrm{S}]_\infty^{*}\frac{k_1}{k_{-1}}\,(4\pi\,Dt)^{-3/2}\,, \tag{63}$$

$$\lim_{t\to\infty}[\mathrm{ES}]^{*} \sim \left([\mathrm{S}]_\infty^{*}\right)^2\frac{k_1}{k_{-1}}\,(4\pi\,Dt)^{-3/2}\,, \tag{64}$$

$$\lim_{\substack{[\mathrm{S}]_0\to 0\\ t\to\infty}}[\mathrm{ES}]^{\mathrm{ran}} \sim \frac{\left(1-[\mathrm{S}]_\infty^{\sigma}\right)k_D[\mathrm{S}]_0}{k_2}\left[1+\left(1-[\mathrm{S}]_\infty^{\sigma}\right)\frac{\sigma}{\sqrt{\pi\,Dt}}\right], \tag{65}$$

$$\lim_{t\to\infty}[\mathrm{S}]^{r_0} \sim [\mathrm{S}]_\infty^{r_0}\left[1+\left(1-[\mathrm{S}]_\infty^{\sigma}\right)\sigma\,(\pi\,Dt)^{-1/2}\right], \tag{66}$$

$$\lim_{t\to\infty}[\mathrm{S}]^{*} \sim [\mathrm{S}]_\infty^{*}\left[1+\left(1-[\mathrm{S}]_\infty^{\sigma}\right)\sigma\,(\pi\,Dt)^{-1/2}\right], \tag{67}$$

$$\lim_{\substack{[\mathrm{S}]_0\to 0\\ t\to\infty}}[\mathrm{S}]^{\mathrm{ran}} \sim 1 - [\mathrm{S}]_0\left(1-[\mathrm{S}]_\infty^{\sigma}\right)k_D t, \tag{68}$$

where $[\mathrm{S}]_\infty^{*}$ is given by equation (33) and

$$[\mathrm{S}]_\infty^{r_0} = \frac{r_0-\sigma}{r_0} + \frac{\sigma}{r_0}\frac{k_2+k_{-1}}{k_{-1}+k_2\,(1+k_1/k_D)}. \tag{69}$$

When $r_0 = \sigma$, the value of $[\mathrm{S}]_\infty^{r_0}$ becomes that of $[\mathrm{S}]_\infty^{\sigma}$.

The relation $[\mathrm{P}] \underset{t\to\infty}{=} 1 - [\mathrm{S}]$ holds because [ES] decreases more rapidly than [S] for both dimensions. Therefore, the long time results of [P] can be obtained from this relation. Interestingly, for the larger initial separation, more ES and S survive at long times.

All the concentrations show universal power-law behaviours in the long time limit, irrespective of the microscopic parameters. The asymptotic power laws for initial random distribution are different from those for initial pair distribution. Interestingly, the $t^{-3/2}$ power-law behaviours of [ES] in 1D and 3D are the same, whereas the long time behaviours of [S] are different since the escape probability is not zero in 3D, confirming Polya's theorem [37]. Note that [P] does not converge to unity in 3D for the same reason.

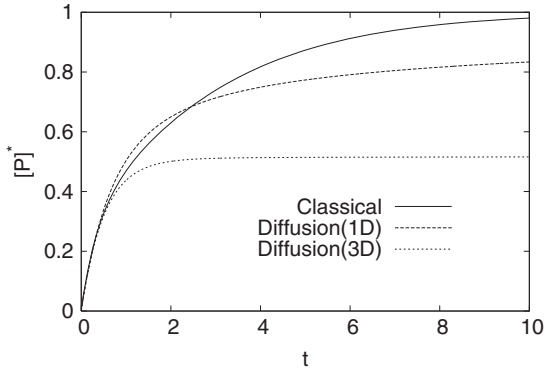

Figure 1. The time dependence of $[P]^*$ for the classical and the diffusion-influenced kinetics in 1D and 3D. The parameter values are $D = 1, \sigma = 1$, and $k_1 = k_{-1} = k_2 = 1$. Note that $[P]^*$ converges to unity in 1D and to 0.519 in 3D.

5. Results and discussions

The numerical solution of the classical kinetics can be easily obtained by solving equations (2)–(4) [43]. In figure 1, we plot a time profile of $[P]^*$ from the numerical solution of the classical kinetics in comparison with those including the diffusion effect in 1D (equation (20)) and 3D (equation (31)). Dimensionless parameters are used as $D = 1, \sigma = 1$, and $k_1 = k_{-1} = k_2 = 1$. Notice that, in 1D, the values of α_i do not depend on σ and so neither does $[P]^*$. The figure shows that the diffusion effect makes the production rate slower in the long time limit in both dimensions. The ultimate yield of the product converges to unity in 1D whereas to a different value of $k_2(1 + k_1/k_D)/[k_{-1} + k_2(1 + k_1/k_D)]$ ($\sim$0.519 for the present parameter set) in 3D, which can be easily seen from the relation $[P] \underset{t\to\infty}{=} 1 - [S]$ and equation (33).

Interestingly, the diffusion effect can make the production rate faster at short times. This can also be explained by the fact that, by stirring the system (for which the diffusion effect is insignificant and the classical kinetics description can usually be employed), a molecule near its reaction partner can escape far away, which leads to the slower reaction rate at short times. In the diffusion-influenced kinetics, the diffusion coefficient (D) and the molecule size (σ) are crucial parameters, whereas the classical kinetics does not depend on them. The dependence of D and σ, however, affects the kinetics differently for the different dimensionality of the media. In 1D (equation (19)) only D affects the reaction, and both D and σ are important in 3D (equation (30)). This point is clearly shown in figure 2, where $[P]^\sigma$ is plotted for two values of $\sigma = 0.1$ and 0.01. Other parameters are the same as in figure 1. While the results of the classical kinetics and 1D results considering diffusion effects are independent of the molecule size, the production rate in 3D becomes faster with decreasing molecule size. Therefore, the product concentration in 3D can be higher than that in 1D at short times. This is an interesting point since [P] is always higher in 1D than in 3D at long times.

We plot the time dependences of the deviation of the substrate concentration $\xi_S(t) \equiv ([S]^\sigma - [S]^\sigma_\infty)/([S]_0 - [S]^\sigma_\infty)$ and that of the enzyme concentration $\xi_E(t) \equiv [E]^\sigma_\infty - [E]^\sigma$ in a log–log scale in figures 3 and 4, respectively. We normalize $\xi_S(t)$ since the value of $[S]^\sigma_\infty$ is not trivial in 3D. The parameter values are the same as in figure 1. In the classical kinetics, the concentrations approach their equilibrium values exponentially while the diffusion effects make the deviations decay with the power-laws. The concentration deviations of the substrate $\xi_S(t)$ and the enzyme $\xi_E(t)$ show the $t^{-1/2}$ and $t^{-3/2}$ asymptotic power-law

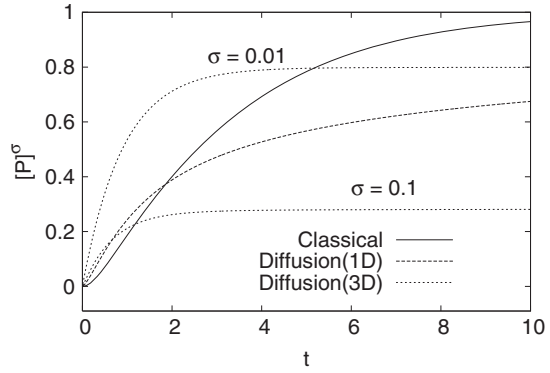

Figure 2. The time dependence of $[P]^{\sigma}$ in 1D and 3D for two values of $\sigma = 0.01$ and $\sigma = 0.1$. The diffusion-influenced kinetics in 1D shows the same behaviour for both values. Other parameter values are the same as in figure 1.

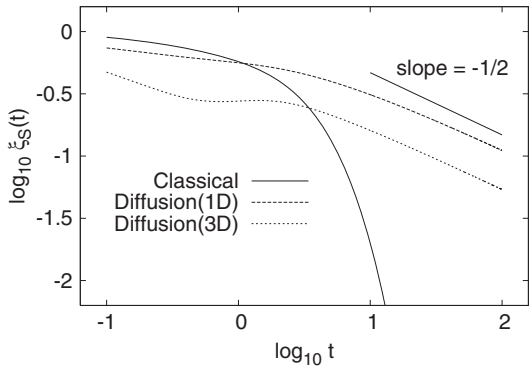

Figure 3. The time dependence of the normalized concentration deviation of substrate, $\xi_S(t) \equiv ([S]^{\sigma} - [S]^{\sigma}_{\infty})/([S]_0 - [S]^{\sigma}_{\infty})$, in a log–log plot for the classical (an exponential decay) and the diffusion-influenced kinetics in 1D and 3D (the power-law decay of $t^{-1/2}$). The parameter values are the same as in figure 1 except $[S]_0 = 1$.

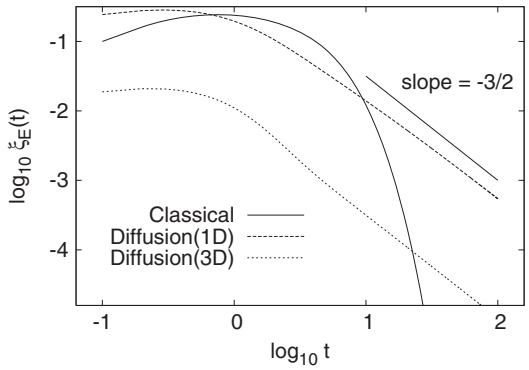

Figure 4. The time dependence of the deviation of enzyme concentration, $\xi_E(t) \equiv [E]^{\sigma}_{\infty} - [E]^{\sigma}$, in a log–log plot for the classical and the diffusion-influenced kinetics in 1D and 3D (the power-law decay of $t^{-3/2}$). The parameter values are the same as in figure 1.

behaviours, respectively, in both dimensions. This is very intriguing because these power-law behaviours are very different from the well known $t^{-d/2}$ behaviour for $A + B \leftrightarrow C$ type reactions in d dimensions [44–47]. These are also different from the $t^{-1/2}$ power-law behaviour for $\xi_E(t)$ previously observed for $[E]_0 \ll [S]_0$ [20].

6. Concluding remarks

We have investigated diffusion-influenced Michaelis–Menten kinetics in the low substrate concentration limit in 1D and 3D. We can obtain the analytical results for the initial pair distribution and for the initial random distribution. The diffusion effect makes the approach to the equilibrium slower by replacing the exponential decay of classical kinetics with the power-law decay. The long time power-law behaviours observed both in 1D and 3D are different from previously reported behaviours. Because of different power-law behaviours of reactants, the intermediate molecules ES disappear faster than the substrate and, therefore, the relation $[P] \underset{t\to\infty}{=} 1 - [S]$ holds at long times.

Qualitative differences between 1D and 3D are found. While the ultimate long time value of $[P]/[E]_0$ is unity in 1D as in the classical kinetics, it is not unity in 3D. The average lifetime of ES is independent of the initial state and depends only on k_2 in 1D, but it depends on the initial state as well as on k_1, k_{-1}, and k_2 in 3D. At short times, the diffusion effect can make the reaction rate faster than that of the classical kinetics, since stirring the system makes a molecule near its reaction partner move far away.

The present results are also applicable to a reaction model similar to Michaelis–Menten kinetics. For example, the following diffusion-influenced protein folding mechanism of the dimeric folding unit [48] can be described by the present results.

$$2E \underset{k_{-1}}{\overset{k_1}{\rightleftharpoons}} E_2 \xrightarrow{k_2} P. \tag{70}$$

Diffusion-influenced enzyme kinetics has often been studied by Monte Carlo simulation methods employing a random walker model on the lattice [11, 17, 49]. However, the relation between the microscopic reaction probability and the phenomenological rate is still ambiguous [50]. This ambiguity prevents the rigorously quantitative comparison between simulation results and the theoretical predictions beyond qualitative comparisons. Brownian dynamics simulations incorporating the exact analytical results are very useful for the quantitative comparison [16, 30–32]. The present exact results provide the algorithm for the Brownian dynamics simulation to obtain numerically exact data for general mechanisms in enzyme kinetics including the competitive or non-competitive inhibition and multi-substrate enzyme systems. The work on the Brownian dynamics simulation will be reported shortly.

Acknowledgment

This work was supported by BK21 Division of Chemistry and Molecular Engineering, Seoul National University.

References

[1] Michaelis L and Menten M L 1913 *Biochem. Z.* **49** 333
[2] Briggs G E and Haldane J B S 1925 *Biochem. J.* **19** 338
[3] Roberts D V 1977 *Enzyme Kinetics* (Cambridge: Cambridge University Press)
[4] Lu H P, Xun L and Xie X S 1998 *Science* **282** 1877

[5] Kou S C, Cherayil B J, Min W, English B P and Xie X S 2005 *J. Phys. Chem.* B **109** 19068
[6] Gopich I and Szabo A 2006 *J. Chem. Phys.* **124** 154712
[7] Rice S A 1985 *Diffusion-Limited Reactions* (New York: Elsevier)
[8] Berg O G, Yu B Z, Rogers J and Jain M K 1991 *Biochemistry* **30** 7283
[9] Gelb M H, Jain M K, Hanel A M and Berg O G 1995 *Annu. Rev. Biochem.* **64** 653
[10] Deutch J M 1998 *J. Chem. Phys.* **108** 937
[11] Kosmidis K, Karalis V, Argyrakis P and Macheras P 2004 *Biophys. J.* **87** 1498
[12] Luby-Phelps K, Castle P, Taylor D and Lanni F 1987 *Proc. Natl Acad. Sci. USA* **84** 4910
[13] Krissinel E B and Agmon N 1996 *J. Comput. Chem.* **17** 1085
[14] Kim H, Shin S and Shin K J 1998 *J. Chem. Phys.* **108** 5861
[15] Kim H, Shin S and Shin K J 1998 *Chem. Phys. Lett.* **291** 341
[16] Kim H, Yang M and Shin K J 1999 *J. Chem. Phys.* **111** 1068
[17] Berry H 2002 *Biophys. J.* **83** 1891
[18] Zhou H-X 1997 *J. Phys. Chem.* B **101** 6642
[19] Yang M, Lee S and Shin K J 1998 *J. Chem. Phys.* **108** 117
[20] Kim H, Yang M, Choi M-Y and Shin K J 2001 *J. Chem. Phys.* **115** 1455 (referred to as I)
[21] Murugan R 2002 *J. Chem. Phys.* **117** 4178
[22] Paul S and Gangopadhyay G 2003 *J. Chem. Phys.* **119** 3501
[23] Miller W G and Alberty R A 1958 *J. Am. Chem. Soc.* **80** 5146
[24] Savageau M A 1995 *J. Theor. Biol.* **176** 115
[25] Zhou H-X 1998 *J. Chem. Phys.* **108** 8146
[26] Sundaram N and Wankat P C 1998 *J. Phys. Chem.* A **102** 717
[27] Molski A 2000 *J. Phys. Chem.* B **104** 4532
[28] Tzafriri A R and Edelman E R 2004 *J. Theor. Biol.* **226** 303
[29] Srere P A 1967 *Science* **158** 936
[30] Edelstein A L and Agmon N 1993 *J. Chem. Phys.* **99** 5396
[31] Kim H, Yang M and Shin K J 1999 *J. Chem. Phys.* **110** 3946
[32] Park S, Shin K J, Popov A V and Agmon N 2005 *J. Chem. Phys.* **123** 034507
[33] Cushman D W and Cheung H S 1976 *Biochim. Biophys. Acta* **424** 449
[34] Marcel V, Palacios L G, Pertuy C, Masson P and Fournier D 1998 *Biochem. J.* **329** 329
[35] Igarashi K, Momohara I, Nishino T and Samejima M 2002 *Biochem. J.* **365** 521
[36] Kim H, Shin S, Lee S and Shin K J 1996 *J. Chem. Phys.* **105** 7705
[37] Polya G 1921 *Math. Ann.* **83** 149
[38] Kim H and Shin K J 1999 *Phys. Rev. Lett.* **82** 1578
[39] Gopich I V and Agmon N 1999 *J. Chem. Phys.* **110** 10433
[40] Kim H, Shin K J and Agmon N 1999 *J. Chem. Phys.* **111** 3791
[41] Huppert D, Goldberg S Y, Masad A and Agmon N 1992 *Phys. Rev. Lett.* **68** 3932
[42] Solntsev K M, Huppert D and Agmon N 2001 *Phys. Rev. Lett.* **86** 3427
[43] Press W H, Flannery B P, Teukolsky S A and Vetterling W T 1988 *Numerical Recipes in C* (Cambridge: Cambridge University Press)
[44] Gopich I V, Ovchinnikov A A and Szabo A 2001 *Phys. Rev. Lett.* **86** 922
[45] Oshanin G S, Ovchinnikov A A and Burlatsky S F 1989 *J. Phys. A: Math. Gen.* **22** L977
[46] Burlatsky S F, Oshanin G S and Ovchinnikov A A 1991 *Chem. Phys.* **152** 13
[47] Burlatsky S F and Oshanin G S 1991 *J. Stat. Phys.* **65** 1095
[48] Gloss L M and Matthews C R 1998 *Biochemistry* **37** 16000
[49] Shea L D, Omann G M and Linderman J J 1997 *Biophys. J.* **73** 2949
[50] Montroll E W and Weiss G H 1965 *J. Math. Phys.* **6** 167